

IGF-I Induces Epithelial-to-Mesenchymal Transition via the IGF-IR-Src-MicroRNA-30a-E-Cadherin Pathway in Nasopharyngeal Carcinoma Cells

Ruoyu Wang,*† Heming Li,† Xuefen Guo,† Zhe Wang,† Shanshan Liang,† and Chengxue Dang*

*Department of Surgical Oncology, The First Affiliated Hospital, Xi'an Jiaotong University College of Medicine, Xi'an, P.R. China

†Department of Oncology, Zhongshan Hospital of Dalian University, Dalian, P.R. China

Recurrence and distant metastasis are the most common cause of therapeutic failure in nasopharyngeal carcinoma (NPC) patients. Insulin-like growth factor I (IGF-I) can induce epithelial-to-mesenchymal transition (EMT) in many epithelial tumors; however, whether IGF-I can enhance NPC metastasis by EMT and the mechanisms remain unclear. Herein, we have identified that IGF-I could induce EMT and enhance migration ability in NPC cell lines. Furthermore, both Src inhibitor and microRNA-30a (miR-30a) inhibitor reversed IGF-I-induced EMT, suggesting the involvement of an IGF-IR-Src-miR-30a-E-cadherin pathway in IGF-I-induced EMT in NPC cell lines. Overall, the results of the present study may provide more useful information regarding the mechanisms of the IGF-IR signaling pathway in the regulation of NPC metastasis. Both Src kinase and miR-30a can be potential biomarkers for selecting high risk of metastasis in NPC patients.

Key words: Epithelial-to-mesenchymal transition (EMT); Insulin-like growth factor I (IGF-I); Insulin-like growth factor I receptor (IGF-IR); Src; MicroRNA-30a (miR-30a)

INTRODUCTION

Nasopharyngeal carcinoma (NPC) is one of the most common malignant diseases in Southeast Asia, especially in southern China (1,2). Despite the initial effectiveness of chemotherapy and radiotherapy, recurrence and distant metastasis are major causes of therapeutic failure in NPC patients (3,4). Contributing to this problem is an incomplete understanding of the mechanisms of metastasis and the lack of effective biomarkers for prediction.

Tumor metastasis is a complex dynamic process involving multiple factors. Recent evidence indicates that epithelial-to-mesenchymal transition (EMT) plays an important role in biological progression and metastasis (5–7). In this process, epithelial cells lose their polarized organization and cell-cell adhesions, undergo cytoskeletal organization, and acquire mesenchymal phenotype (8). With regard to the molecular mechanisms of EMT, the insulin-like growth factor-I receptor (IGF-IR)/ligand system has been identified to initiate EMT progression and increase the metastatic potential of prostate, breast, and gastric cancer cells (6,9,10). Consistently, a clinical study has identified that IGF-IR is overexpressed in NPC patients with lymph node or distant metastasis (11). However, whether IGF-I can enhance NPC metastasis by EMT and the mechanisms remain unclear.

Besides growth factors, microRNAs (miRNAs) have also been suggested as regulatory molecules in EMT progression in different cancers (12–14). miRNAs are small noncoding small RNAs that are 19–25 nucleotides long and contribute to the regulation of their target genes through mRNA degradation or translation inhibition (15). Recently, it was indicated that miR-30a inhibited EMT and invasion in breast and lung cancer (16,17). However, Wang et al. reported that miR-30a promoted invasiveness and metastasis through EMT in NPC (18). Therefore, the role of miR-30a in EMT progression still remains unclear and needs further investigation.

In the present study, we revealed that IGF-I could induce EMT and enhance migration ability in NPC cell lines. Furthermore, an IGF-IR-Src-miR-30a-E-cadherin pathway existed in IGF-I-induced EMT in NPC cell lines.

MATERIALS AND METHODS

Cell Cultures

Human NPC cell lines (CNE2 and Hone1) were received as a gift from the Guangzhou Medical University of China. All the cells were cultured in medium RPMI-1640 (Gibco, USA) supplemented with 10% fetal bovine serum (Gibco), penicillin (100 U/ml), and streptomycin (100 mg/ml) in a humidified incubator at 37°C with 5% CO₂.

Reagents and Antibodies

Recombinant human IGF-I was purchased from R&D System (Wiesbaden, Germany). OSI-906, the dual IGF-IR/IR inhibitor, was purchased from SelleckBio (Houston, TX, USA). PP2 was purchased from Sigma-Aldrich (St. Louis, MO, USA). Antibodies to E-cadherin, vimentin, IGF-IR, phospho-IGF-IR (Tyr1131), Src, and phospho-Src (Y416) were purchased from Cell Signaling Technology Inc. (Beverly, MA, USA). Anti-actin and secondary goat anti-rabbit and goat anti-mouse antibodies were purchased from Santa Cruz Biotechnology Inc. (Santa Cruz, CA, USA).

Western Blot Assay

The cells were washed three times with ice-cold 1× phosphate-buffered saline (PBS). Total protein was extracted using the radioimmunoprecipitation assay (RIPA) lysis buffer (Beyotime Institute of Biotechnology, Haimen, China) according to the manufacturer's instructions. All the samples were eluted by boiling water at 100°C for 5 min with 3X sampling buffer. For Western blot analysis, equal amounts of protein samples (10–20 µg) were separated by 10% SDS-polyacrylamide gel electrophoresis (SDS-PAGE) and electronically transferred to polyvinylidene difluoride (PVDF) membranes (Millipore, Billerica, MA, USA). After blocking with 5% skim milk in TBST (Beyotime Institute of Biotechnology), the blots were incubated with appropriate primary antibodies at 4°C overnight. The next day, the blots were incubated with monoclonal anti-rabbit or mouse secondary antibodies (Santa Cruz Biotechnology Inc.) for 30 min at room temperature. After washing with TBST, proteins were visualized by enhanced chemiluminescence reagent (ECL; Cell Signaling Technology). The values are representative of at least three independent experiments.

Migration Assays

For the Transwell migration assays, 1×10^4 CNE2 and Hone1 cells were plated on the top chamber with a noncoated membrane (24-well insert; 8-µm pore size; Corning) with 200 µl of serum-free RPMI-1640 medium with or without IGF-I (100 ng/ml). The upper chamber was inserted into a 24-well culture dish with a medium supplemented with 10% serum. After incubation for 48 hours, the nonmigrated cells were removed from the upper sides of the Transwell membrane with a cotton swab. The migrated cells on the lower sides were stained with crystal violet, and the cells were counted in five different fields at 10× magnification under the microscope.

Quantitative Real-Time PCR (qPCR) Assay

Total DNA was extracted with TRIzol reagent (Invitrogen, USA). For miRNAs, miRcute miRNA First-Strand cDNA Synthesis kit (Tiangen Biotech, Beijing, China) was

used for RNA reverse transcription. Expression of miRNA-30a (miR-30a) was detected by SYBR Green quantitative polymerase chain reaction (PCR) amplifications kit (Tiangen Biotech) and measured by the QuantStudio 7 Flex Real-Time PCR System (Applied Biosystems, USA). Relative expression of miRNA was calculated via the comparative cycle threshold (Ct) method, and the expression of U6 small nuclear RNA was used as reference. The sequence-specific forward primer for miR-30a was 5'-GACGGTACCTGGTGGAGAACAACTTCG-3', and for U6 was 5'-GCTTCGGCAGCACATATACTAAAAT-3' (forward) and 5'-CGCTTCACGAATTGCGTGTCA-3' (reverse), respectively. The PCR conditions were 30 s at 95°C, followed by 45 cycles at 95°C for 5 s and 58°C for 34 s.

Statistical Analysis

All data were analyzed using SPSS 19.0 software (SPSS, Chicago, IL, USA). Differences in measurement data were presented as mean±standard deviation. Comparison between the two groups was analyzed using *t*-test. A value of *p*<0.05 was defined as statistically significant.

RESULTS

IGF-I Induces EMT in CNE2 and HONE-1 NPC Cells

To elucidate the role of IGF-I in NPC cells, cultured CNE2 and HONE-1 cells were treated with human recombinant IGF-I (100 ng/ml) for 48 h after overnight serum starvation according to a previous study (10). Figure 1A presents the dramatic morphological change after IGF-I treatment in NPC cells lines. Most of the cells lost tight cell-cell junctions, became scattered, and the mesenchymal cell shape became elongated. Furthermore, significant downregulation of the epithelial marker E-cadherin and upregulation of mesenchymal marker vimentin were observed under Western blot compared with the control groups (Fig. 1B). Additionally, cellular migration ability was promoted after IGF-I treatment, with $58 \pm 1.5\%$ treated versus $12 \pm 3.6\%$ control for CNE2 cells (*p*<0.05) and $52 \pm 4.0\%$ treated versus $17 \pm 1.2\%$ control for Hone1 cells (*p*<0.05) (Fig. 1C). These data indicated that IGF-I could induce EMT and promote cellular migration ability in CNE2 and Hone1 NPC cells.

IGF-I-Induced EMT Was Regulated by the Src Signaling Pathway

Given that the Src signaling pathway mediates EMT progression and promotes metastasis in several tumor cells, we further examined the activation level of the Src signaling pathway in CNE2 and Hone1 after IGF-I stimulation. As shown in Figure 2A, the phosphorylation levels of IGF-IR and Src were detected at 3 min and increased time dependently by IGF-I stimulation. To elucidate whether IGF-I-induced

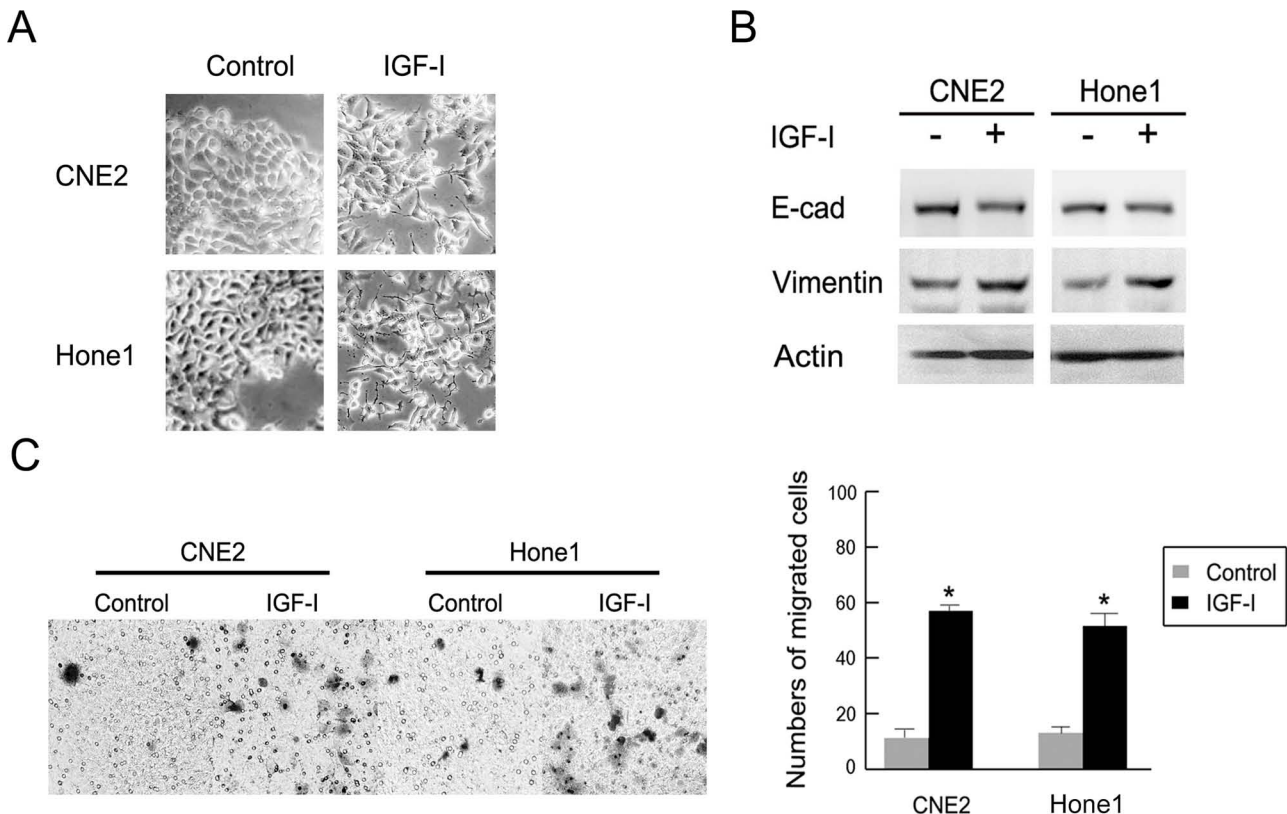


Figure 1. IGF-I induced EMT and enhanced the cellular migration ability in NPC cells. CNE2 and Hone1 cells were treated with or without IGF-I (100 ng/ml) for 48 h after being serum starved overnight. (A) Photos were taken at 20× magnification. (B) EMT markers E-cadherin and vimentin were detected by Western blot analysis. (C) Migration ability of CNE2 and Hone1 cells after IGF-I (100 ng/ml) treatment are shown. The indicated values reflect the mean±standard deviation (SD) from three independent experiments. E-cad, E-cadherin; Vim, vimentin. *IGF-I untreated versus IGF-I treated, $p<0.05$.

EMT was dependent on the Src signaling pathway, NPC cells were pretreated with the IGF-IR/IR inhibitor OSI-906 (10 μ M) or Src inhibitor PP2 (10 μ M) for 2 h to block the signaling pathways before IGF-I stimulation according to previous studies (19,20). As shown in Figure 2B, the phosphorylation level of the Src signaling pathway was inhibited after pretreatment with OSI-906 or PP2 followed by IGF-I stimulation. Meanwhile, CNE2 cells did not exhibit either morphological changes or EMT marker switching after pretreatment with signaling pathway-specific inhibitor (Fig. 2C and D). These results indicated that IGF-I-induced EMT was maybe in part due to the activation of the downstream Src signaling pathway in NPC cells.

MicroRNA-30a Was Involved in IGF-I-Induced EMT in NPC Cells

Previous studies indicated that miR-30a played variable roles in the EMT process in different tumor cells. To figure out its effect on IGF-I-induced EMT in NPC cells, we detected the relative miR-30a levels after IGF-I treatment under quantitative PCR analysis. As shown in Figure 3A, the relative level of miR-30a was increased by

more than 2.5 times in CNE2 cells following IGF-I treatment for 48 h compared with the control group ($p<0.05$). The levels of miR-30a expression were downregulated significantly after transfection with miR-30a inhibitor in CNE2 cells (Fig. 3B). Furthermore, the cells exhibited a dramatic morphological change after miR-30a inhibitor transfection in combination with IGF-I stimulation, from elongated and scattered mesenchymal cells to characteristic epithelial cells with tight junctions each other (Fig. 3C). Similarly, we also observed that EMT markers switching was partially reversed after inhibition of miR-30a under IGF-I treatment obviously (Fig. 3D). These results indicate that miR-30a could partially repress IGF-I-induced EMT in NPC cells.

Src Signaling Pathway Regulated MicroRNA-30a Expression in IGF-I-Induced EMT in NPC Cells

To identify the associations between the Src signaling pathway and miR-30a, we pretreated CNE2 cells with Src inhibitor PP2 (10 μ M) for 2 h to block the signaling pathways before IGF-I stimulation. As shown in Figure 4, PP2 partially reversed miR-200c downregulation after

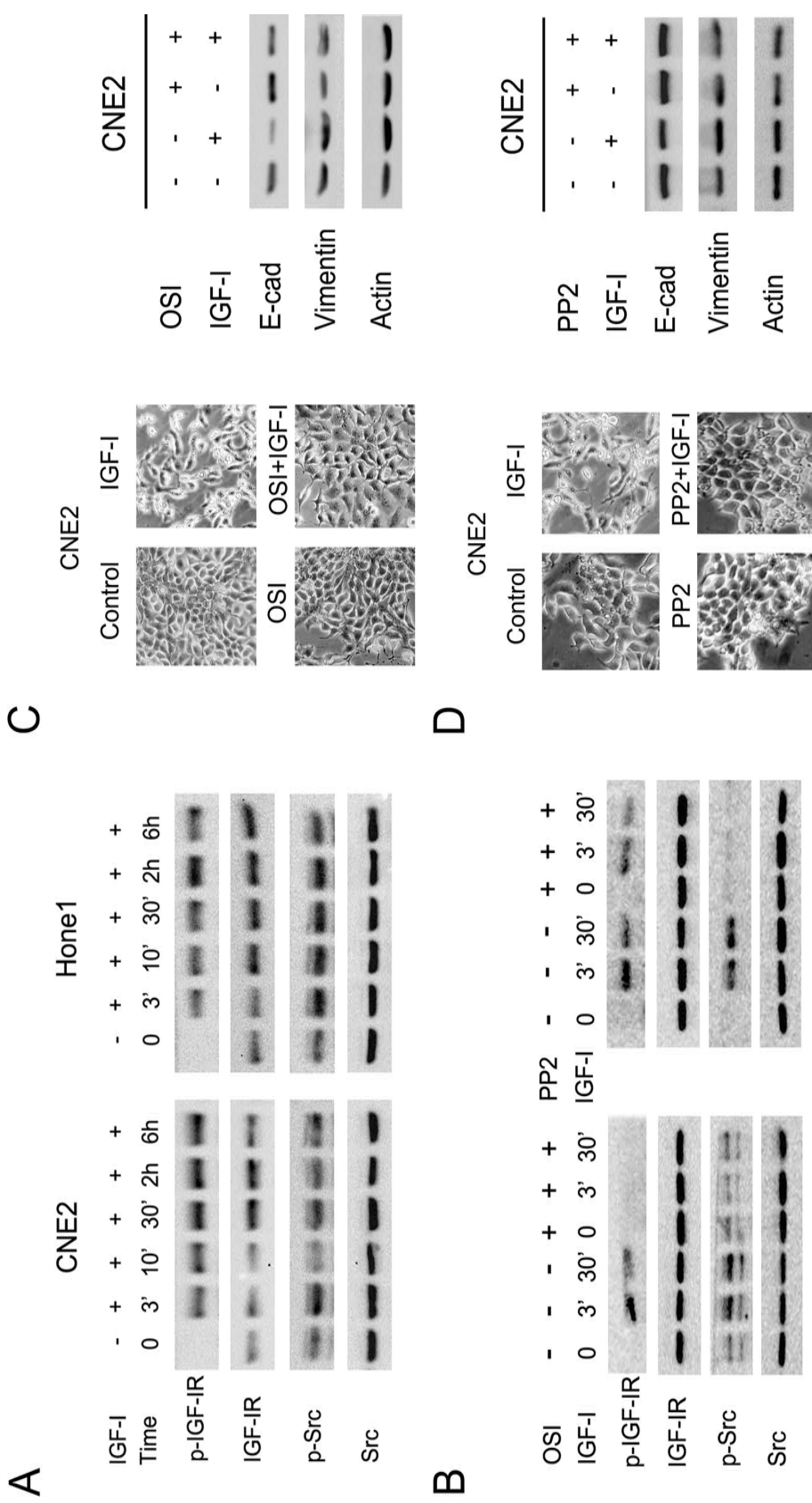


Figure 2. IGF-I activated Src downstream signaling pathways and induced EMT in NPC cells. (A) The serum-starved CNE2 and Hone1 cells were incubated with IGF-I (100 ng/ml) for the indicated times, and the phosphorylation of IGF-IR and Src was analyzed by Western blot. (B) The serum-starved cells were pretreated with or without OSI-906 (10 μ M) or PP2 (10 μ M) for 2 h followed by IGF-I (100 ng/ml) stimulation for the indicated times, and the phosphorylation of IGF-IR and Src was analyzed by Western blot. (C, D) The serum-starved cells were pretreated with or without OSI-906 (10 μ M) or PP2 (10 μ M) for 2 h followed by IGF-I (100 ng/ml) stimulation for 48 h. Cell lysates were collected for Western blot analysis. Photos were taken at 20 \times magnification. E-cad, E-cadherin; OSI, OSI-906.

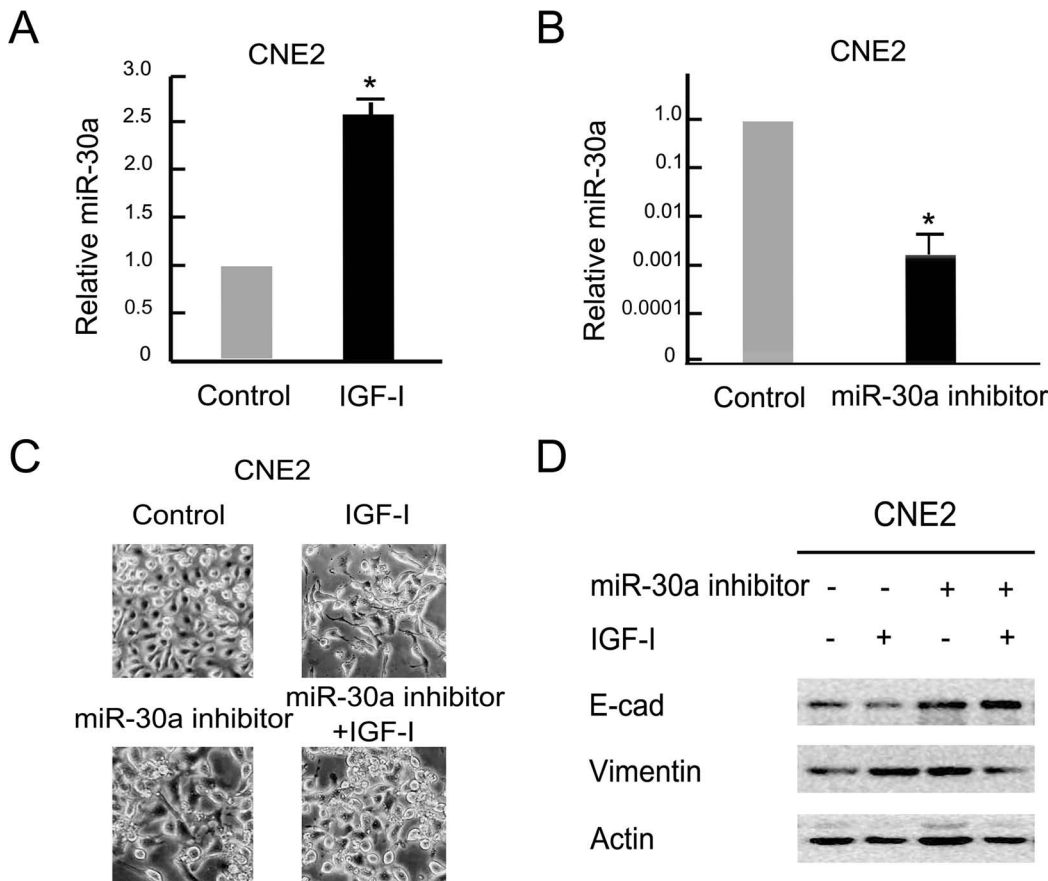


Figure 3. Inhibition of miR-30a repressed IGF-I-induced EMT in NPC cells. (A) The serum-starved CNE2 cells were treated with IGF-I (100 ng/ml) for 48 h. The expression of miR-30a was analyzed by real-time polymerase chain reaction (PCR). Data are mean \pm SD from three independent experiments. Control group as reference. *IGF-I untreated versus IGF-I treated, $p < 0.05$. (B) miR-30a inhibitor was transfected into CNE2 cells for 48 h. The expression of miR-30a was analyzed by real-time PCR. Data are mean \pm SD from three independent experiments. Control transfected versus miR-30a inhibitor transfected, $p < 0.05$. (C, D) The serum-starved cells were transfected with or without the miR-30a inhibitor for 48 h followed by IGF-I (100 ng/ml) stimulation for 48 h. Cell lysates were collected for Western blot analysis. Photos were taken at 20 \times magnification. E-cad, E-cadherin.

IGF-I stimulation. This result indicated that the Src signaling pathway could regulate miR-30a expression after IGF-I-induced EMT progression in NPC cells.

DISCUSSION

Despite significant progress in NPC, invasion and metastasis are still the leading cause of mortality, especially for patients with a high risk of metastasis. Elucidation of the molecular mechanisms underlying metastasis is crucial to improve the survival rates for advanced NPC. In the present study, we reported for the first time that IGF-I could induce EMT and enhance cellular migration ability in NPC cell lines. Additionally, inhibition of Src signaling pathway could reverse IGF-I-induced EMT progression. Interestingly, the activation of the Src signaling pathway upregulated the relative level of miR-30a expression and downregulated E-cadherin expression. These results

suggested that an IGF-IR–Src–miR-30a–E-cadherin pathway existed in IGF-I-induced EMT progression in NPC.

Recently, several study groups have reported that IGF-I induces EMT and promotes tumor cell invasion and migration ability. For example, Yao et al. reported IGF/STAT3/NANOG/Slug signaling axis controls EMT and stemness maintenance in colorectal cancer (21). Our group used this to demonstrate that IGF-I-induced EMT via GSK-3 β (glycogen synthase kinase-3 β) and ZEB2 in the BGC-823 gastric cancer cell line (6). In addition, ubiquitin ligase Cbl-b repressed IGF-I-induced EMT via ZEB2 and miR-200c regulation in gastric cancer cells (5). However, whether IGF-I could induce EMT in NPC cells is still not clear. In the present study, we reported for the first time that IGF-I could induce EMT and enhance cellular migration ability in NPC cell lines via the Src signaling pathway.

Src is a nonreceptor, cytoplasmic, tyrosine kinase, which can be activated following stimulation of receptor tyrosine

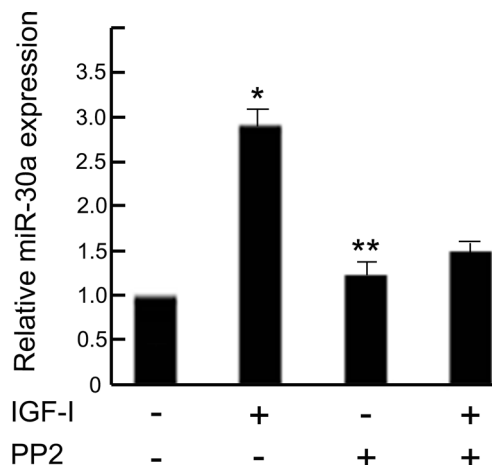


Figure 4. Inhibition of the Src signaling pathway repressed IGF-I-induced upregulation of miR-30a expression in NPC cells. The serum-starved cells were pretreated with or without PP2 (10 μ M) for 2 h followed by IGF-I (100 ng/ml) stimulation for 48 h. The expression of miR-30a was analyzed by real-time PCR. Control group as reference. *IGF-I untreated versus IGF-I treated; **In IGF-I treated group, PP2 unpretreated versus PP2 pretreated, $p < 0.05$.

kinases in many tumors (22). There is evidence of Src kinase in tumor progression-related events such as EMT and the development of metastasis. Avizienyte et al. reported that activation of Src, via its SH2 and SH3 domains, induced the EMT by deregulating E-cadherin and inhibiting its function, while at the same time promoting assembly of integrin adhesion structures to promote a mesenchymal state (23). Our group used this to find that Src was an important mediator for IGF-IR activation in cetuximab resistance in gastric cancer cells (19). Ke et al. reported that aberrant activation of Src facilitated NPC cells with metastatic ability through activation of the PI3K/Akt pathway and induction of the EMT process (20). However, this study first identified that ligand IGF-I could activate Src signaling pathway and induce EMT in NPC cell lines, which further elucidated the new mechanism of the Src signaling pathway in IGF-I-induced EMT.

There has been increasing evidence of miR-30a in the regulation of tumor metastasis, but the results seem inconsistent. Chang et al. demonstrated that miR-30a increased tight junction protein expression and suppressed EMT in breast cancer (16). In addition, miR-30a inhibited EMT by targeting Snail in non-small cell lung cancer (17). Downregulation of miR-30a facilitated tumor cell migration, invasion, and EMT progression in hepatocellular cancer (24). However, Wang et al. demonstrated that miR-30a was identified to promote EMT process by targeting the E-cadherin gene in NPC metastasis (18). Furthermore, our study acquired the same result that miR-30a increased EMT progression in NPC cells. These results indicate that miR-30a may play different biological roles in variant tumor cells. In addition,

we further demonstrated a new mechanism for miR-30a in the EMT process, which was an IGF-IR–Src–miR-30a–E-cadherin pathway in IGF-I-induced EMT in NPC cells. Therefore, this result may provide more evidence on miR-30a in the regulation of NPC metastasis.

CONCLUSION

In summary, our study suggests that IGF-I induces the EMT process in NPC cells. An IGF-IR–Src–miR-30a–E-cadherin pathway is involved in IGF-I-induced EMT in NPC cells. These results provide more evidence of the mechanisms of IGF-IR signaling pathway in the regulation of NPC metastasis. Both Src kinase and miR-30a can be a potential biomarker for selecting a high risk of metastasis in NPC patients. However, highly informative prospective clinical studies are needed for further investigation.

ACKNOWLEDGMENT: This work was supported by grants from the National Natural and Scientific Foundation of China (No. 30970869 and No. 81502124).

REFERENCES

- Wei, W. I.; Sham, J. S. Nasopharyngeal carcinoma. *Lancet* 365(9476):2041–2054; 2005.
- Guigay, J. Advances in nasopharyngeal carcinoma. *Curr. Opin. Oncol.* 20(3):264–269; 2008.
- Tham, I. W.; Hee, S. W.; Yeo, R. M.; Salleh, P. B.; Lee, J.; Tan, T. W.; Fong, K. W.; Chua, E. T.; Wee, J. T. Treatment of nasopharyngeal carcinoma using intensity-modulated radiotherapy—The National Cancer Centre Singapore experience. *Int. J. Radiat. Oncol. Biol. Phys.* 75(5):1481–1486; 2009.
- Liu, N.; Jiang, N.; Guo, R.; Jiang, W.; He, Q. M.; Xu, Y. F.; Li, Y. Q.; Tang, L. L.; Mao, Y. P.; Sun, Y. MiR-451 inhibits cell growth and invasion by targeting MIF and is associated with survival in nasopharyngeal carcinoma. *Mol. Cancer* 12(1):123; 2013.
- Li, H.; Xu, L.; Li, C.; Zhao, L.; Ma, Y.; Zheng, H.; Li, Z.; Zhang, Y.; Wang, R.; Liu, Y. Ubiquitin ligase Cbl-b represses IGF-I-induced epithelial mesenchymal transition via ZEB2 and microRNA-200c regulation in gastric cancer cells. *Mol. Cancer* 13(1):1; 2014.
- Li, H.; Xu, L.; Zhao, L.; Ma, Y.; Zhu, Z.; Liu, Y.; Qu, X. Insulin-like growth factor-I induces epithelial to mesenchymal transition via GSK-3 β and ZEB2 in the BGC-823 gastric cancer cell line. *Oncol. Lett.* 9(1):143–148; 2015.
- Lee, J. M.; Dedhar, S.; Kalluri, R.; Thompson, E. W. The epithelial-mesenchymal transition: New insights in signaling, development, and disease. *J. Cell Biol.* 172(7):973–981; 2006.
- Thompson, E. W.; Newgreen, D. F. Carcinoma invasion and metastasis: A role for epithelial-mesenchymal transition? *Cancer Res.* 65(14):5991–5995; 2005.
- Graham, T. R.; Zhau, H. E.; Odero-Marah, V. A.; Osunkoya, A. O.; Kimbro, K. S.; Tighiouart, M.; Liu, T.; Simons, J. W.; O'Regan, R. M. Insulin-like growth factor-I-dependent up-regulation of ZEB1 drives epithelial-to-mesenchymal transition in human prostate cancer cells. *Cancer Res.* 68(7):2479–2488; 2008.
- Walsh, L. A.; Damjanovski, S. IGF-1 increases invasive potential of MCF7 breast cancer cells and induces activation

- of latent TGF- β 1 resulting in epithelial to mesenchymal transition. *Cell Commun. Signal.* 9(1):10; 2011.
11. Yuan, Y.; Zhou, X.; Song, J.; Qiu, X.; Li, J.; Ye, L.; Meng, X.; Xia, D. Expression and clinical significance of epidermal growth factor receptor and type 1 insulin-like growth factor receptor in nasopharyngeal carcinoma. *Ann. Otol. Rhinol. Laryngol.* 117(3):192–200; 2008.
 12. Wang, N.; Wang, Q.; Shen, D.; Sun, X.; Cao, X.; Wu, D. Downregulation of microRNA-122 promotes proliferation, migration, and invasion of human hepatocellular carcinoma cells by activating epithelial-mesenchymal transition. *Onco. Targets Ther.* 9:2035–2047; 2016.
 13. Yoo, J. O.; Kwak, S. Y.; An, H. J.; Bae, I. H.; Park, M. J.; Han, Y. H. miR-181b-3p promotes epithelial–mesenchymal transition in breast cancer cells through Snail stabilization by directly targeting YWHAG. *Biochim. Biophys. Acta* 1863(7):1601–1611; 2016.
 14. Chen, Q.; Jiao, D.; Wang, J.; Hu, H.; Tang, X.; Chen, J.; Mou, H.; Lu, W. miR-206 regulates cisplatin resistance and EMT in human lung adenocarcinoma cells partly by targeting MET. *Oncotarget*; 2016.
 15. Chen, X.; Ba, Y.; Ma, L.; Cai, X.; Yin, Y.; Wang, K.; Guo, J.; Zhang, Y.; Chen, J.; Guo, X. Characterization of microRNAs in serum: A novel class of biomarkers for diagnosis of cancer and other diseases. *Cell Res.* 18(10):997–1006; 2008.
 16. Chang, C. W.; Yu, J. C.; Hsieh, Y. H.; Yao, C. C.; Chao, J. I.; Chen, P. M.; Hsieh, H. Y.; Hsiung, C. N.; Chu, H. W.; Shen, C. Y. MicroRNA-30a increases tight junction protein expression to suppress the epithelial-mesenchymal transition and metastasis by targeting Slug in breast cancer. *Oncotarget* 7(13):16462–16478; 2016.
 17. Kumarswamy, R.; Mudduluru, G.; Ceppi, P.; Muppala, S.; Kozlowski, M.; Niklinski, J.; Papotti, M.; Allgayer, H. MicroRNA-30a inhibits epithelial-to-mesenchymal transition by targeting Snai1 and is downregulated in non-small cell lung cancer. *Int. J. Cancer* 130(9):2044–2053; 2012.
 18. Wang, H. Y.; Li, Y. Y.; Fu, S.; Wang, X. P.; Huang, M. Y.; Zhang, X.; Shao, Q.; Deng, L.; Zeng, M. S.; Zeng, Y. X. MicroRNA-30a promotes invasiveness and metastasis in vitro and in vivo through epithelial-mesenchymal transition and results in poor survival of nasopharyngeal carcinoma patients. *Exp. Biol. Med. (Maywood)* 239(7):891–898; 2014.
 19. Li, X.; Xu, L.; Li, H.; Zhao, L.; Luo, Y.; Zhu, Z.; Liu, Y.; Qu, X. Cetuximab-induced insulin-like growth factor receptor I activation mediates cetuximab resistance in gastric cancer cells. *Mol. Med. Rep.* 11(6):4547–4554; 2015.
 20. Ke, L.; Xiang, Y.; Guo, X.; Lu, J.; Xia, W.; Yu, Y.; Peng, Y.; Wang, L.; Wang, G.; Ye, Y. c-Src activation promotes nasopharyngeal carcinoma metastasis by inducing the epithelial-mesenchymal transition via PI3K/Akt signaling pathway: A new and promising target for NPC. *Oncotarget*; 2016.
 21. Yao, C.; Su, L.; Shan, J.; Zhu, C.; Liu, L.; Liu, C.; Xu, Y.; Yang, Z.; Bian, X.; Shao, J. IGF/STAT3/NANOG/Slug signaling axis simultaneously controls epithelial-mesenchymal transition and stemness maintenance in colorectal cancer. *Stem Cells* 34(4):820–831; 2016.
 22. Bromann, P. A.; Korkaya, H.; Courtneidge, S. A. The interplay between Src family kinases and receptor tyrosine kinases. *Oncogene* 23(48):7957–7968; 2004.
 23. Avizienyte, E.; Fincham, V. J.; Brunton, V. G.; Frame, M. C. Src SH3/2 domain-mediated peripheral accumulation of Src and phospho-myosin is linked to deregulation of E-cadherin and the epithelial-mesenchymal transition. *Mol. Biol. Cell* 15(6):2794–2803; 2004.
 24. Liu, Z.; Tu, K.; Liu, Q. Effects of microRNA-30a on migration, invasion and prognosis of hepatocellular carcinoma. *FEBS Lett.* 588(17):3089–3097; 2014.